Journal of Non-Crystalline Solids 359 (2013) 1–4

Contents lists available at SciVerse ScienceDirect

Journal of Non-Crystalline Solids

journal homepage: www.elsevier.com/locate/jnoncrysol

Giant magnetocaloric effect in Tm-based bulk metallic glasses

J.T. Huo [a], D.Q. Zhao [a], H.Y. Bai [a], E. Axinte [b], W.H. Wang [a,*]

[a] *Institute of Physics, Chinese Academy of Sciences, Beijing 100190, P. R. China*
[b] *Gheorghe Asachi Technical University of Iasi, Faculty of Machine Manufacturing and Industrial Management, 700500 Iasi, Romania*

A R T I C L E I N F O

Article history:
Received 21 May 2012
Received in revised form 7 September 2012
Available online xxxx

Keywords:
Metallic glass;
Entropy change;
Giant magnetocaloric effect;
Candidate for magnetic refrigerants

A B S T R A C T

We report that the maximum magnetic entropy change ΔS_m of $Tm_{39}Ho_{16}Co_{20}Al_{25}$ metallic glass can reach 18.3 $Jkg^{-1}\ K^{-1}$ under 5 T, which is larger than that of any previously reported metallic glasses and comparable with that of the giant magnetocaloric effect material $Gd_5Si_2Ge_2$ compound. Even under low magnetic field of 2 T, the ΔS_m of the glass can reach 10.3 $Jkg^{-1}\ K^{-1}$ which is even larger that of most of other metallic glasses under 5 T. The excellent magnetocaloric effect and refrigerant efficiency together with unique mechanical and physical properties of the metallic glasses indicate they are promising candidate for magnetic refrigerants.

1. Introduction

The last few decades have seen a continuous increase of interest in the magnetocaloric effect (MCE) and magnetic refrigeration [1]. Compared with conventional vapor-cycle refrigeration, the magnetic refrigeration techniques based on the MCE have advantages of both high energy efficiency and environmentally friendliness [2]. The magnitude of the magnetocaloric effect is given by the field induced entropy change (ΔS_m) due to the alignment of its magnetic spins that occurs on exposure to an external magnetic field [3]. To satisfy practical application, extensive efforts have been carried out to pick out promising materials exhibiting large MCE as magnetic refrigerants.

Since the discovery of so-called giant MCE in the ternary compound $Gd_5Si_2Ge_2$ [4], there is incentive from both fundamental and practical points of view to explore large MCE in crystalline rare earth compounds and materials possessing a first-order structural and magnetic phase transitions, which leads to a giant magnetic field-induced entropy change, across their ordering temperature. A series of such materials with large even giant MCE such as Gd-Co-Si [5], Mn-Fe-P-As-Ge [6], La-Na-K-MO_3 [7], and Ni-Mn-Ga [8] have been obtained.

Very recently, the MCE in a series of heavy rare earth (Gd, Tb, Dy, Ho and Er) based bulk metallic glasses (BMGs) have been investigated [9–14]. It has been found that these BMGs manifested large MCE over much wider temperature range, and directly lead to a much higher refrigerant capacity (RC), which is an important parameter that characterizes the refrigerant efficiency of a material. Their unique properties associated with their intrinsic nature, such as the tailorable ordering temperature, the higher electrical resistivity and thus the smaller eddy current heating, high corrosion resistance, outstanding mechanical properties, and high thermally stability, manifest their promising application as candidate for magnetic refrigerants. However, the ΔS_m values of these BMGs are not comparable to that of crystalline compound $Gd_5Si_2Ge_2$. Therefore exploring new BMGs with much larger ΔS_m especially under relative low magnetic field is particularly important to improve the efficiency of the material used as refrigerant.

In this work, the MCE of a series of Tm-based BMGs under a modest magnetic field has been investigated. The ΔS_m of these BMGs, especially $Tm_{39}Ho_{16}Co_{20}Al_{25}$ BMG, is turned out to be far larger than that of the previous reported rare earth based BMGs and comparable to that of the giant MCE material of $Gd_5Ge_2Si_2$. Our work shows that the BMGs appear to be candidate for the active magnetic refrigerants working in helium and hydrogen liquefaction temperature range.

2. Experiments

The Tm-based BMGs with nominal compositions $Tm_{39}RE_{16}Co_{20}Al_{25}$ (RE = Ce, Pr, Nd, Sm, Gd, Tb, Dy, Ho and Er) were prepared by arc melting pure Tm, Ce, Pr, Nd, Sm, Gd, Tb, Dy, Ho, Er, Co and Al in a Ti-gettered argon atmosphere. The ingot was remelted and suck-cast into a Cu mold to get a cylindrical rod 3 mm in diameter. Their amorphous nature was ascertained by x-ray diffraction (XRD) using a MAC Mo3 XHF diffractometer with Cu $K\alpha$ radiation. Thermal analysis was carried out in a Perkin-Elmer DSC-7 differential scanning calorimeter (DSC). The temperature and field dependences of magnetization were measured in a SQUID magnetometer (Quantum Design).

3. Results

Fig. 1 shows the XRD patterns of the as-cast Tm-based BMGs. The board diffraction peaks and no appreciable peaks indicate that full

* Corresponding author. Fax: +86 10 82640223.
E-mail address: whw@iphy.ac.cn (W.H. Wang).

0022-3093/$ – see front matter © 2012 Elsevier B.V. All rights reserved.
http://dx.doi.org/10.1016/j.jnoncrysol.2012.09.020

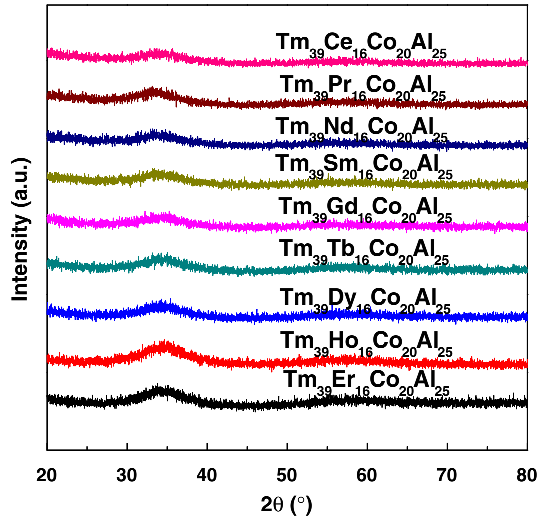

Fig. 1. XRD patterns of the as-cast $Tm_{39}RE_{16}Co_{20}Al_{25}$ (RE = Ce, Pr, Nd, Sm, Gd, Tb, Dy, Ho and Er) BMGs (diameter is 3 mm).

glassy rods can be obtained for the alloys at least 3 mm in diameter. The glassy feature was further confirmed by DSC trace as shown in Fig. 2. It can be seen that an endothermic reaction due to glass transition occurs followed by one or two sharp two exothermic peaks due to the multi-process of crystallization. The glass transition temperature (T_g), first crystallization temperature (T_{x1}) and supercooled liquid region $\Delta T = T_{x1} - T_g$ at the heating rate of 20 K/min are listed in Table 1. The ΔT, one of the important parameters in evaluating the glass-forming ability (GFA) of an alloy, of $Tm_{39}Nd_{16}Co_{20}Al_{25}$ is 80 K, which is larger than the other rare earth based BMGs as shown in Table 1. The distinctive glass transition and sharp crystallization events as well as large values of ΔT further confirm the excellent GFA of these alloys. It is also found that the T_g increases as the atomic number of the substituting element increases. Young's modulus E and T_g have an empirical correlation of $T_g = 2.5E$. [15] Therefore, the

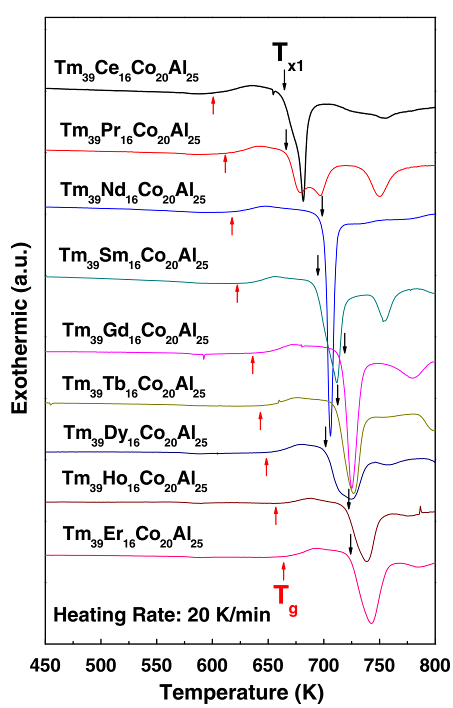

Fig. 2. DSC curves of the as-cast $Tm_{39}RE_{16}Co_{20}Al_{25}$ (RE = Ce, Pr, Nd, Sm, Gd, Tb, Dy, Ho and Er) BMGs. The scanning rate is 20 K/min.

increasing can be attributed to the increasing E of the substituting elements.

Fig. 3(a) presents the temperature dependence of the magnetization (M–H) determined in an applied field of 200 Oe for $Tm_{39}Ho_{16}Co_{20}Al_{25}$ BMG. The zero field cooling (ZFC) branch was measured on heating after initially cooling from 300 to 2 K in zero field. The field cooling (FC) branch was measured on heating after initially cooling to 2 K in the same measuring field. From the FC curves a spin freezing transition can clearly be seen, while in the ZFC curve a cusp is observed at the same temperature where divergence appeared between the FC and the ZFC branches showing typical spin-glass-like behavior [14]. Although the strong disorder effect exists in the amorphous sample, it can be seen that the magnetization varies sharply at the ordering temperature. According to the Maxwell relation, the sharp variation of magnetization near the transition temperature T_f indicates large magnetic entropy for this alloy [12]. The T_f of the alloy determined from the ZFC curve is 4.2 K, and the T_f for the other eight BMGs has also been measured and listed in Table 1. It can bee seen that the transition temperature can be tuned easily in large temperature range below 20 K by alloying different rare earth element in the Tm-based BMGs. The advantage of wide choice of alloy compositions available in the Tm-based BMGs makes them an attractive choice for refrigerants in multistage magnetic refrigerators.

A set of isothermal magnetization curves of M–H with increasing filed in a large temperature range for the $Tm_{39}Ho_{16}Co_{20}Al_{25}$ BMG is displayed in the inset of Fig. 3(a). In the vicinity of T_f the temperature step of 1 or 2 K was chosen, and a step of 5 K for the regions far away from T_f. The sweeping rate of field is slow enough to ensure the data are recorded in an isothermal process. In an isothermal process of magnetization, the total magnetic entropy change of the system due to the application of a magnetic field can be derived from Maxwell relation by integrating over the magnetic field [16]:

$$\Delta S_m(T,H) = \int_{H\min}^{H\max} \left(\frac{\partial M}{\partial T}\right)_H dH, \tag{1}$$

where H_{min} and H_{max} represent the initial and final values of magnetic field, respectively. Minimum value of zero and maximal value of 5 T of the magnetic field was fixed in our experiments. To derive the temperature dependence of magnetic entropy change, the numerical approximation of the integral is usually applied [17]:

$$\Delta S_m = \sum_i \frac{M_i - M_{i+1}}{T_i - T_{i+1}} \Delta H, \tag{2}$$

where M_i and M_{i+1} are the experimental values of the magnetization at T_i and T_{i+1} under an applied magnetic field H_i respectively. By measuring the isothermal M–H curves at various temperatures, the magnetic entropy change associated with the H variation can be evaluated according to Eq. (2). Fig. 3(b) shows the $-\Delta S_m$ as a function of temperature under 2 and 5 T for the $Tm_{39}Ho_{16}Co_{20}Al_{25}$ BMG. The peak value of $-\Delta S_m$ under 5 T is 18.3 $Jkg^{-1}\,K^{-1}$ at 11 K, which is comparable with that of $Gd_5Ge_2Si_2$ (18.6 $Jkg^{-1}\,K^{-1}$) [4], so-called giant MCE material and considered as good magnetic refrigerant. This value is also much larger than that of previous glassy materials reported, such as Gd-based BMGs (~7.6–9.5 $Jkg^{-1}\,K^{-1}$) [9,10], Tb-based BMGs (7.5 $Jkg^{-1}\,K^{-1}$) [11], Dy-based BMGs (9.5 $Jkg^{-1}\,K^{-1}$) [12], Ho-based BMGs (11.8 $Jkg^{-1}\,K^{-1}$) [13], Er-based BMGs (15.9 $Jkg^{-1}\,K^{-1}$) [14] and Pd-based BMGs (0.58 $Jkg^{-1}\,K^{-1}$) [18]. Fig. 4 presents a comparison of the $-\Delta S_m$ of Tm-based BMG, other reported BMGs and crystalline magnetic refrigerants under 5 T. It can be seen distinctly that the largest value of the $-\Delta S_m$ among the amorphous materials has been obtained in the Tm-based BMGs. Under 2 T, the peak slightly moves to lower temperature and narrows compared with that of 5 T, but the peak value can reach 10.3 $Jkg^{-1}\,K^{-1}$ for $Tm_{39}Ho_{16}Co_{20}Al_{25}$ BMG. This value is much higher than those of previously reported results

Table 1
Magnetic entropy changes upon allying a field H of Tm-based BMGs, various materials [1,3,4,9–14,18] and related parameters. *a* and *c* stand for the amorphous and crystalline states, respectively.

Composition	Structure	T_g (K) (±1 K)	T_{x1} (K) (±1 K)	ΔT (K) (±1 K)	Applied field (T)	Transition temperature (K) (±1 K)	$-\Delta S_m$ ($Jkg^{-1}\ K^{-1}$) (±0.1 $Jkg^{-1}\ K^{-1}$)	RC (Jkg^{-1})
$Tm_{39}Ce_{16}Co_{20}Al_{25}$	a	608	663	55	5	2.0	14.8	207
$Tm_{39}Pr_{16}Co_{20}Al_{25}$	a	611	666	55	5	2.0	14.5	208
$Tm_{39}Nd_{16}Co_{20}Al_{25}$	a	621	701	80	5	4.0	12.2	182
$Tm_{39}Sm_{16}Co_{20}Al_{25}$	a	631	693	62	5	7.0	11.3	178
$Tm_{39}Gd_{16}Co_{20}Al_{25}$	a	646	717	71	5	10.5	11.2	340
$Tm_{39}Tb_{16}Co_{20}Al_{25}$	a	650	711	61	5	12	9.9	248
$Tm_{39}Dy_{16}Co_{20}Al_{25}$	a	657	701	44	5	5.0	12.6	283
$Tm_{39}Ho_{16}Co_{20}Al_{25}$	a	666	719	53	5	4.0	18.3	333
$Tm_{39}Er_{16}Co_{20}Al_{25}$	a	668	723	55	5	3.0	18.1	301
$Gd_{53}Al_{24}Co_{20}Zr_3$	a	599	653	54	5	93.0	9.4	590
$Gd_{51}Al_{24}Co_{20}Zr_4Nb_1$	a	598	653	55	5	91.0	9.2	651
$Tb_{55}Co_{20}\ Al_{25}$	a	614	680	66	5	45.0	7.5	375
$Dy_{36}Ho_{20}Al_{24}Co_{20}$	a	633	687	54	5	23.0	9.5	326
$Ho_{36}Dy_{20}Al_{24}Co_{20}$	a	553	629	76	5	17.0	11.8	365
$Er_{50}Al_{24}Co_{20}Y_6$	a	651	702	51	5	8.0	15.9	423
$Pd_{40}Ni_{22.5}Fe_{17.5}P_{20}$	a	600	666	66	5	94.0	0.6	87
Gd	c	–	–	–	5	293.0	9.8	–
$Gd_5Si_2Ge_2$	c	–	–	–	5	276.0	18.6	306
$Gd_5Si_2Ge_{1.9}Fe_{0.1}$	c	–	–	–	5	276.0	7.0	360
$MnFeP_{0.45}As_{0.55}$	c	–	–	–	5	306.0	18.3	390

for compounds with the same field variation of 2 T, such as $ErAl_2$ (~5 $Jkg^{-1}\ K^{-1}$) [19], $La(Fe_{1-x}Co_x)Fe_{11.83}Al_{1.17}$ (~4.8 $Jkg^{-1}\ K^{-1}$) [20] and $Tb_xY_{1-x}Al_2$ (1.2–7.6 $Jkg^{-1}\ K^{-1}$) [21], and even comparable with that of most of other metallic glasses found under 5 T (see Table 1). The results show that we have developed novel magnetic materials displaying larger MCEs under lower fields of about 2 T, which can be generated by permanent magnets. The giant magnetic entropy change combining excellent glass formation ability, considerable higher elastic modulus, smaller Poisson's ratio, high mechanical strength, and intrinsic brittleness of Tm-based BMGs might promote the practical applications of metallic glasses as a magnetic refrigerant [22–24].

Fig. 5(a) shows the $-\Delta S_m$ as a function of temperature for $Tm_{39}RE_{16}Co_{20}Al_{25}$ (RE = Ce, Pr, Nd, Sm, Gd, Tb, Dy, Ho and Er) BMGs under 5 T. One can find that the $-\Delta S_m$ of the Tm-based BMGs is larger due to the larger magnetic moment of Tm and the peaks in the magnetic entropy change are broad due to fluctuation of the exchange integral [10]. It can be seen, with the change of the element, the value and width of the peaks changes indicating that the glassy refrigerants can work in different temperature range by choosing different substituting elements. The $Tm_{39}Gd_{16}Co_{20}Al_{25}$ BMG has the widest peak, and the $Tm_{39}Ho_{16}Co_{20}Al_{25}$ BMG is the highest peak. The ΔS_m of the Tm-based BMGs is strongly dependent on the theoretical molar magnetic S_M of the substituting rare earth element. The S_M is proportional to the total orbital quantum number J and is given by $S_M = R\ln(2J+1)$, where R is the gas constant [25]. The largest J of Ho during the lanthanide atom brings $Tm_{39}Ho_{16}Co_{20}Al_{25}$ the largest ΔS_m in this series of Tm-based BMGs as shown in Fig. 5(b).

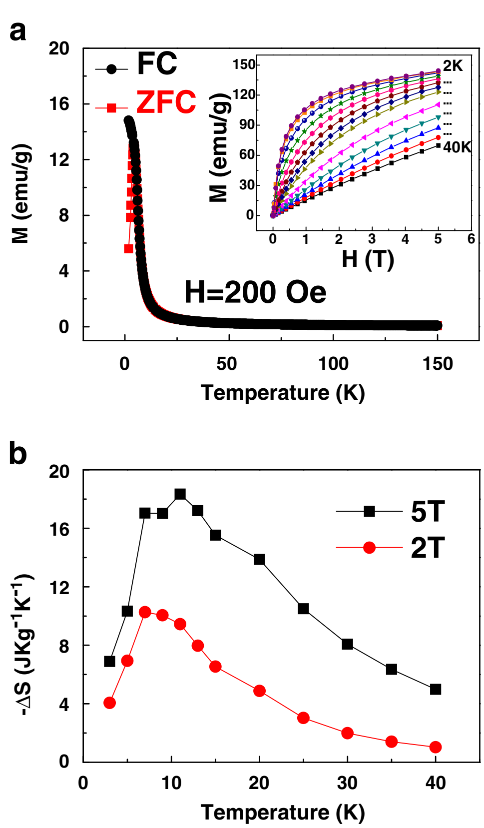

Fig. 3. (a) Temperature dependence of the ZFC and FC magnetization under a magnetic field of 200 Oe. (b) Magnetic entropy changes as a function of temperature under 2 and 5 T for $Tm_{39}Ho_{16}Co_{20}Al_{25}$ BMG. The inset shows the isothermal magnetization as a function of magnetic field at various temperatures for this alloy.

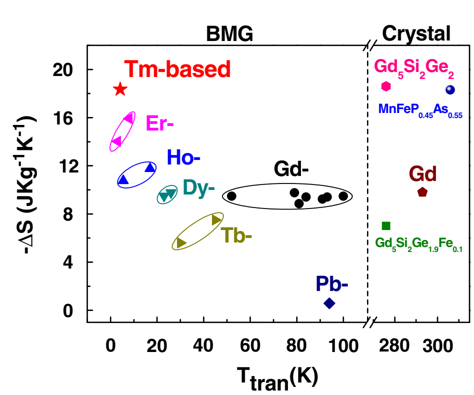

Fig. 4. A comparison of the magnetic entropy changes ($-\Delta S_m$) under 5 T and transition temperature (T_{tran}) among Tm-based BMG, other reported BMGs and crystalline magnetic refrigerants.

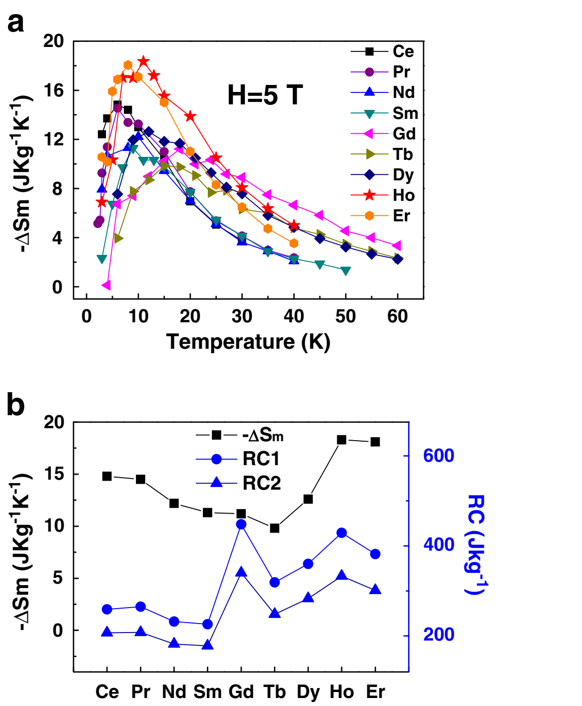

Fig. 5. (a) Magnetic entropy changes as a function of temperature under 5 T. (b) Composition dependence of the magnetic entropy changes ($-\Delta S_m$), the refrigerant capacity RC1 and RC2 for $Tm_{39}RE_{16}Co_{20}Al_{25}$ (RE = Ce, Pr, Nd, Sm, Gd, Tb, Dy, Ho and Er) BMGs.

4. Discussion

The magnetic refrigerant efficiency can also be characterized by the refrigerant capacity (RC), which is proportional to the area under the $-\Delta S_m$ versus T curve. The RC of the Tm-based BMGs was estimated by two methods. The first involves taking the direct product of the maximum entropy change and the full width at half-maximum (FWHM) of the peak [26]. The other is obtained by numerically integrating the area under the ΔS_m-T curve, using the temperatures at half-maximum of the peak as the integration limits [11,27–29]. The RC values achieved by the first method (RC1) for $Tm_{39}Gd_{16}Co_{20}Al_{25}$ and $Tm_{39}Ho_{16}Co_{20}Al_{25}$ are determined to be 448 (Jkg^{-1}) and 429 (Jkg^{-1}), respectively. The RC values achieved by the second method (RC2) for $Tm_{39}Gd_{16}Co_{20}Al_{25}$ and $Tm_{39}Ho_{16}Co_{20}Al_{25}$ are 340 (Jkg^{-1}) and 333 (Jkg^{-1}), respectively. These values are comparable with those of $Gd_5Si_2Ge_2$ (305 Jkg^{-1}) and $Gd_5Si_2Ge_{1.9}Fe_{0.1}$ (360 Jkg^{-1}) [18], indicating the better refrigerant efficiency of the Tm-based BMGs. The high RC is due to the larger magnetic entropy change and the glassy structure which extends the large MCE into wider temperature range. The composition dependence of the RC1 and RC2 for $Tm_{39}RE_{16}Co_{20}Al_{25}$ (RE = Ce, Pr, Nd, Sm, Gd, Tb, Dy, Ho and Er) BMGs was shown in Fig. 5(b). As one can see the change regularity of the RC obtained by the two methods correspond very well despite that the RC2 is a little smaller than RC1. It is obvious that the RC of Tm-based BMGs substituted by heavy rare earth element is larger than that of Tm-based BMGs substituted by light rare earth element.

5. Conclusions

The giant MCE has been observed in Tm-based BMGs. The maximum value of the magnetic entropy change of $Tm_{39}Ho_{16}Co_{20}Al_{25}$ BMG can reach 10.26 $Jkg^{-1}\,K^{-1}$ under 2 T and 18.34 $Jkg^{-1}\,K^{-1}$ under 5 T respectively, which can compare favorably with that of $Gd_5Si_2Ge_2$ and is the largest value during the glassy materials. The transition temperature, magnetic entropy change and refrigerant capacity are tunable by changing the substituting elements. The excellent refrigerant capacity due to giant magnetic entropy change together with other merits of the metallic glasses make Tm-BMGs suitable candidate for use as magnetic refrigerant.

Acknowledgement

This work was supported by MOST 973 of China (Nr. 2010CB731603) and the National Natural Science Foundation of China (Nrs. 50731008 and 50921091).

References

[1] V.K. Pecharsky, K.A. Gschneidner Jr., J. Magn. Magn. Mater. 200 (1999) 44.
[2] O. Tegus, E. Bruck, K.H.J. Buschow, F.R. de Boer, Nature 415 (2002) 150.
[3] V. Provenzano, A.J. Shapiro, R.D. Shull, Nature 429 (2004) 853.
[4] V.K. Pecharsky, K.A. Gschneidner Jr., Phys. Rev. Lett. 78 (1997) 4494.
[5] M. El-Hagary, H. Michor, G. Hilscher, J. Magn. Magn. Mater. 322 (2010) 2840.
[6] O. Tegus, B. Fuquan, W. Dagula, L. Zhang, E. Bruck, P.Z. Si, F.R. de Boer, K.H.J. Buschow, J. Alloy Compd. 396 (2005) 6.
[7] Y. Regaieg, M. Koubaa, W.C. Koubaa, A. Cheikhrouhou, T. Mhiri, J. Alloy Compd 502 (2010) 270.
[8] S.K. Srivastava, V.K. Srivastava, R. Chatterjee, Solid State Commun. 152 (2012) 372.
[9] (a) Q. Luo, D.Q. Zhao, M.X. Pan, W.H. Wang, Appl. Phys. Lett. 89 (2006);
(b) Q. Luo, W.H. Wang, J. Non-Cryst. Solids 355 (2009) 759.
[10] Q. Luo, W.H. Wang, J. Alloy Compd. 495 (2010) 209.
[11] Y.T. Wang, H.Y. Bai, M.X. Pan, D.Q. Zhao, W.H. Wang, Sci. China G 51 (2008) 337.
[12] L. Liang, X. Hui, C.M. Zhang, G.L. Chen, J. Alloy. Compd. 463 (2008) 30.
[13] H. Fu, X.T. Zu, H.J. Yu, X.T. Zu, Solid State Commun. 145 (2008) 15.
[14] Q. Luo, D.Q. Zhao, M.X. Pan, W.H. Wang, Appl. Phys. Lett. 90 (2007) 211903.
[15] (a) W.H. Wang, J. Appl. Phys. 99 (2006) 093506;
(b) W.H. Wang, J. Appl. Phys. 110 (2011) 053521;
(c) Y.H. Liu, C.T. Liu, W.H. Wang, A. Inoue, T. Sakurai, M.W. Chen, Phys. Rev. Lett. 103 (2009) 065504;
(d) W.H. Wang, Prog. Mater. Sci. 57 (2012) 487.
[16] T. Hashimoto, T. Numasawa, M. Shino, T. Okada, Cryogenics 21 (1981) 647.
[17] R.D. McMichael, J.J. Ritter, R.D. Shull, J. Appl. Phys. 73 (1993) 6946.
[18] T.D. Shen, R.B. Schwarz, J.Y. Coulter, J.D. Thompson, J. Appl. Phys. 91 (2002) 5240.
[19] P.J. von Ranke, V.K. Pecharsky, K.A. Gschneidner Jr., Phys. Rev. B 58 (1998) 12110.
[20] F.X. Hu, B.G. Shen, J.R. Sun, Z.H. Cheng, Phys. Rev. B 64 (2001) 012409.
[21] X. Bohigas, J. Tejada, F. Torres, J.I. Arnaudas, E. Joven, A. del Moral, Appl. Phys. Lett. 81 (2002) 2427.
[22] H.B. Yu, P. Yu, W.H. Wang, H.Y. Bai, Appl. Phys. Lett. 92 (2008) 141906.
[23] W.H. Wang, Adv. Mater. 21 (2009) 4524.
[24] E. Axinte, Mater. Des. 35 (2011) 518.
[25] K.A. Gschneidner Jr., A.O. Pecharsky, V.K. Pecharsky, Cryocoolers 12 (2003) 457.
[26] K.A. Gschneidner, V.K. Pecharsky, A.O. Pecharsky, C.B. Zimm, Mater. Sci. Forum 69 (1999) 315.
[27] V. Franco, J.M. Borrego, A. Conde, S. Roth, Appl. Phys. Lett. 88 (2006) 132509.
[28] J. Yi, L.S. Huo, D.Q. Zhao, M.X. Pan, H.Y. Bai, W.H. Wang, Sci. China G 54 (609) (2012).
[29] J.F. Li, J.Q. Wang, X.F. Liu, H.Y. Bai, M.X. Pan, W.H. Wang, Sci. China G 53 (2010) 409.